IEEE Access
Multidisciplinary | Rapid Review | Open Access Journal

Received March 30, 2022, accepted April 18, 2022, date of publication May 2, 2022, date of current version May 5, 2022.

Digital Object Identifier 10.1109/ACCESS.2022.3170452

Study of Multiobjective Genetic Algorithm on Taylor External Fixation

JIANMIN GUO AND JIALONG SU
School of Computer Science and Technology, Tiangong University, Tianjin 300387, China
Corresponding author: Jianmin Guo (guojianmin@tiangong.edu.cn)

This work was supported in part by the major social science projects of the Tianjin Education Commission under Grant 2017JW2D28.

ABSTRACT The rapid development of today's society and the rapidly increasing incidence of skeletal injuries caused by traffic and industrial accidents have led to a significant increase in the number of patients with fractures accompanied by severe soft tissue injuries, as well as an increased incidence of osteomyelitis and bone defects. Many of these patients cannot be treated with internal fixators and can only be treated with external fixators. The Taylor Bone External Fixator is the most advanced bone external fixation brace in the field of orthopedics, in which the algorithm study of the forward and backward solution of the computer software that accompanies the Taylor Bone External Fixator is the key. In this paper, we analyze the positional kinematic model based on the Taylor Spatial Frame and derive the equations for solving the six positional parameters of the fracture segment in the dynamic platform with this model. A multi-objective genetic algorithm and Pareto optimization theory are combined to propose a solution to the kinematic positive solution problem. The algorithm proposed in this paper has a minimum accuracy improvement of about 0.8 mm compared to the conventional Newton-Raphson in terms of the accuracy of the Taylor frame mounting parameters solution. Finally, based on the human tibial fracture as the test object, the healing process of the tibial fracture end was simulated using the prescription data generated by the orthopedic system, and the experimental results proved the accuracy and feasibility of the software system, and achieved the expected orthopedic effect.

INDEX TERMS Taylor bone external fixator, multi-objective genetic algorithm, Pearson correlation coefficient, kinematic positive solution, correction prescription.

I. INTRODUCTION

The term ''bone external fixator'' was introduced by European orthopedic surgeon Albin Lambotte, who designed a bone suture device in 1990. Albin Lambotte fixes multiple steel nails with a spiral pattern outside the fracture segment and controls the depth of the nails in the segment by constant adjustment to correct the morphology of the bone segment. In recent years, there has been an increase in the number of fractures and orthopedic arthropathies caused by traffic accidents and workplace injuries [1], and the open reduction internal fixation technique for limb fractures requires an incision of the patient's fracture site, and internal fixation cannot be performed in cases where the fracture segment is severely damaged or the bone segment is deformed. In this case, the Taylor Spatial Frame (TSF) technique of external bone fixation has shown good healing rates in clinical practice [2] and is one of the main modalities used in orthopedics in medical institutions, with the characteristics of a small incision, stable correction, simple and easy to operate orthopedic method, effective prevention of cartilage tissue and nerve strain damage, and few postoperative complications [3].

Most of the current algorithms for solving positive and negative solutions of the kinematic platform in Taylor bone external fixator structures use traditional numerical, including the Newton-Raphson method, the modified Jacobi matrix method, and some local optimization algorithms. However, the kinematic positive solution process has a high number of iteration steps when solving the deformation parameters and a high dependence on the initial values [4], which is very likely to cause the poor accuracy of the feasible solutions. In the clinical of TSF, even millimeter-level parameter errors can cause the prescription data of subsequent orthopedic treatment to be less accurate. It is also based on this problem that makes it difficult to apply and develop TSF in the actual orthopedic treatment.

The associate editor coordinating the review of this manuscript and approving it for publication was Liangxiu Han.

Due to the many advantages offered by TSF, this similar framework model has been studied in many literatures. The study in [5] implements a fast and efficient evolutionary algorithm for solving the kinematic positive solution problem of a 6-degree-of-freedom frame consisting of a non-planar, non-symmetric fixed and moving platform. The authors use inverse kinematics to formulate this through a system of position-based equations to maximize the reduction of errors in platform movement. A new approach to the kinematic positive solution of the Stewart platform with additional sensors is proposed in [6], where the magnitude of the position vector can be measured by an additional sensor. The authors in [7] propose a neural network-based kinematic solution method for parallel robots, using a novel network model to optimize the computational accuracy.

In addition, the process of solving the kinematic positive solution of the machine platform involves 12 sets of 6-dimensional nonlinear equations [8], and it is extremely difficult to obtain the optimal feasible solution of this multi-objective optimization problem. Furthermore, by examining recent studies, it can be hypothesized that previous studies targeting similar TSF frameworks have not focused on considering fixed-point coordinate models incorporating the human skeleton and lack visualization to simulate the process of skeletal correction. In this paper, the key technologies related to the Taylor Bone External Fixator Orthotic System are investigated and a set of mathematical models for the fixed-point coordinates of digital images and the kinematic solution of the TSF platform structure are established.

Based on these explanations, the main contributions of this paper are summarized as follows:

For the first time, the multi-objective genetic algorithm was creatively combined into the Taylor Bone external fixation orthopedic system platform, which solved the current problems of difficulty in solving the deformity posture parameters and the accuracy of the solved result parameters.

To facilitate the verification of the accuracy and feasibility of the multi-objective genetic algorithm in the study of Taylor bone external fixation correction, a software system of correction prescription was designed at the later stage of the experiment, and the kinematic orthogonal solution algorithm combined with the idea of the multi-objective genetic algorithm was embedded into the software system to verify the accuracy and feasibility of the study through the visualization interface operation. This is another innovation of this paper, which has not been addressed in any previous study.

II. RELATED WORK

In 1994, orthopedic surgeon J. Charles Taylor combined the Chasles axis theory and the projective geometry based on the Stewart-Gough platform to link six freely rotatable and retractable metal support rods between rings with a rigid structure to form the Taylor Bone Fixation Brace, which is now used in orthopedic surgeries referred to as the TSF Bone Fixator. The TSF structure based on the Stewart-Gough platform fills the gap in the theoretical design of medical device structures in the field of orthopedics [9] and is characterized by a strong and adjustable fixator and high accuracy of orthopedic prescription data. By calculating the deformation pose parameters of the fracture segment and coordinating the length change of the six retractable rods, the spatial position of the dynamic and static platform can be adjusted by changing the scale value of support rods. In clinical practice, this method allows dynamic and static platforms in the TSF structure to reach the ideal position for the orthopedic treatment of the fracture segment.

A. TAYLOR BONE EXTERNAL FIXATOR STRUCTURE

The TSF structure derives from the Stewart-Gough platform mechanism [10], and the overall frame structure of TSF consists of two orthopedic platforms (including the dynamic platform Q and the static platform P) and six retractable rods marked with graduated values (in millimeters). To apply to different skeletal orthopedic scenarios, non-regular rings with different inner diameter specifications are available for each platform. The schematic structure of the fixator and its components are shown in Figure 1(a). The 3D simulation illustration of the structure is shown in Figure 1 (b), blue color indicates the dynamic platform Q, gray color indicates the static platform P, and the 6 retractable rods are assigned to 6 different colors.

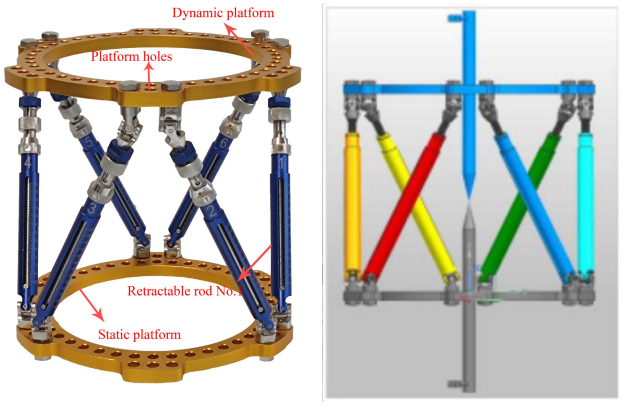

FIGURE 1. Schematic illustration of the TSF structure.

The dynamic and static platforms and the six retractable rods are interconnected by Hooke hinges through the platform holes [5], forming six connection points at the top and the bottom respectively, to form a fixation effect on the retractable rods. When the static platform is fixed to the patient's fracture site, we assume that the static platform will not produce displacement and angular offset difference during the kinematic solution of the whole orthopedic system, which means that the lower static platform of the orthopedic system will not change its position once installed during the whole orthotic cycle of the patient. By examining the current patient's treatment process in the field, we found that the static platform does take into account during the orthopedic

treatment phase to try not to deflect its position and angle, which is precisely determined by the structural properties of the Taylor frame. Therefore, the static platform P will be used as the base coordinate system of the algorithm during the kinematic solution of the dynamic and static platform, the coordinate systems of other positions will be modeled and calculated using P-xyz as the reference. The six retractable rods between the dynamic platform and the static platform are numbered from 1 to 6 in the clockwise order. They are rendered in red, orange, yellow, green, cyan, and blue respectively, and each rod is marked with a scale value representing retraction range as well as accuracy, as shown in Figure 1(b). To ensure the adjustability of the orthopedic system data, the scale value range of the telescopic rod is also changed according to different skeleton correction scenarios.

B. TAYLOR PLATFORM POSE KINEMATIC MODEL

The focus of this paper is to find a suitable computational approach to solve the parametric problem of the kinematic positive solution based on the TSF structure. For this calculation, we propose to consider two dimensions: the efficiency (time) of solving the parameters and the accuracy of the parameter results. Two concepts related to kinematic solution algorithms are involved, the kinematic inverse solution algorithm and the kinematic positive solution algorithm. The kinematic inverse solution algorithm means that the position and attitude of the dynamic platform are known and the amount of motion of the drive is calculated. For this paper, the movement of the actuator is the amount of expansion and contraction of the six struts compared to the initial length. The kinematic positive solution algorithm refers to solving the position and attitude of the dynamic platform of the TSF mechanism platform with known lengths of its six struts. The Taylor bone external fixator is composed of two dynamic and static platform structures and six scalable telescopic rods. Only by adjusting the scale values corresponding to the six freely movable telescopic rods respectively can the positional data of the dynamic platform obtained from the positive solution algorithm be reflected in the mathematical model. From the definition of kinematic positive and negative solutions, it is easy to see that the process of solving kinematic positive and negative solutions is reciprocal, and since the inverse solution algorithm is much easier than the positive solution algorithm, later studies of the positive solution algorithm can use the inverse solution algorithm to verify the accuracy and feasibility of the results.

The process of solving kinematic positive solution values of the Taylor bone external fixator can be viewed as an optimization problem of solving a multivariate objective function, which falls within the scope of operations research. For this solution process, the research strategy of this paper is to set it as a set of six-element nonlinear equations to solve optimally, and we can set a set of nonlinear equations according to the parameters of the initial attitude of the measured dynamic platform, and the optimal solution found in its feasible solution domain is a set of unique and optimal positional parameters for the positive kinematic solution of the Taylor bone external fixator, an idea we follow from Pareto optimization theory.

First of all, the coordinate system of the dynamic platform is set as Q, and its three-dimensional coordinate system is u, v, w, which is defined as the moving coordinate system $Q - uvw$. The corresponding coordinate system of the static platform is P with three-dimensional coordinate systems x, y, z, and is defined as the base coordinate system $P - xyz$. The point P is the geometric center of the static platform, Q is the geometric center of the dynamic platform, the six positions of the dynamic platform connected to the hinge are set as N1, N2, N3, N4, N5, N6, and the six positions of the static platform connected to the hinge are set as M1, M2, M3, M4, M5, M6. The specific simple coordinate structure of the Taylor bone external fixator is schematically shown in Figure 2.

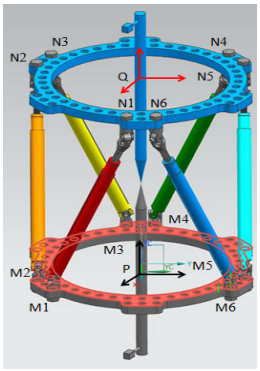

FIGURE 2. Coordinate structure diagram of TSF.

The static platform is always stationary compared to the dynamic platform because of the structural properties of the Taylor frame, so the static coordinate system P is at relative rest for the dynamic coordinate system Q [6]. To reduce the unnecessary parameters generated during the solving process, the positive direction of the x-axis in the static coordinate system P is set as the midpoint of M1 and M2, the direction of the z-axis is set perpendicular to the horizontal plane of the base, the positive direction of the y-axis can be obtained by the right-hand rule. In the coordinate system of the moving stage $Q - uvw$, the positive direction of each axis is kept parallel and in the same direction as the static stage. We can understand that the coordinate system $Q-uvw$ of the dynamic platform is obtained by the upward vertical projection of the static platform coordinate system $P - xyz$.

In the dynamic platform coordinate system, the angle of rotation around the x-axis is denoted as α, the angle of rotation around the y-axis is denoted as β, the angle of rotation around the z-axis is denoted as γ, and the three-dimensional spatial angle attitude coordinates of the dynamic platform in the coordinate system can be obtained as (α, β, γ).

The vertical projection of the movable and static platforms of the immobilizer shows that the graph formed by the connection points of the six hinges and platforms has a non-positive hexagonal distribution, we can abstract the structural schematic shown in Figure 2 into a mathematical geometric model, as shown in Figure 3. The angle of rotation in the coordinate system can be calculated from the offset angle formed by the fracture and the vector displacement of the line segment [11].

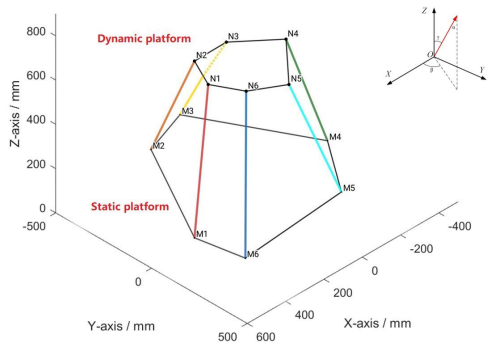

FIGURE 3. Taylor rack geometry model.

During the movement of the Taylor frame, both the connecting rod and the dynamic platform will generate complex movements. But if we consider these objects as rigid bodies, then we can describe their poses in space in the same way that we describe the position and pose of a rigid body in space. We describe it in a Cartesian coordinate system with the top view of the Taylor frame shown in Figure 4, where a_i is the radius of the dynamic platform and b_i is the radius of the static platform.

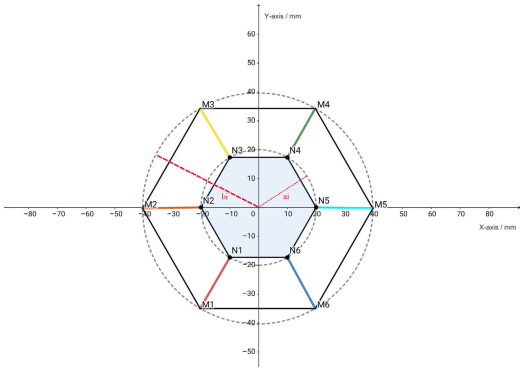

FIGURE 4. Top view of Taylor rack.

If the rotation angle of the dynamic platform Q around the static platform P-x axis in the bone external fixator is recorded as α, the bone part can be approximated as a line at this point, and the corresponding matrix can be obtained by the formula

$$\begin{bmatrix} x \\ y \\ z \end{bmatrix} = R \begin{bmatrix} x' \\ y' \\ z' \end{bmatrix} \tag{1}$$

The coordinate conversion calculation is performed, and the coordinate conversion matrix of its rotation angle α can be expressed as

$$R\,(\mathrm{x}, \alpha) = \begin{bmatrix} 1 & 0 & 0 \\ 0 & \cos\alpha & -\sin\alpha \\ 0 & \sin\alpha & \cos\alpha \end{bmatrix} \tag{2}$$

Similarly, when the rotation angles of a point A in the dynamic platform Q of the bone external fixator around the static platform P-y axis and P-z axis are β and γ, respectively, the specific matrix representation of each rotation angle can be obtained as

$$R(y, \beta) = \begin{bmatrix} \cos\beta & 0 & \sin\beta \\ 0 & 1 & 0 \\ -\sin\beta & 0 & \cos\beta \end{bmatrix} \tag{3}$$

$$R(z, \gamma) = \begin{bmatrix} \cos\gamma & -\sin\gamma & 0 \\ \sin\gamma & \cos\gamma & 0 \\ 0 & 0 & 1 \end{bmatrix} \tag{4}$$

Equation (2), Equation (3), and Equation (3) are already known, then the calculation process of projecting the coordinate system Q of the dynamic platform into the coordinate system P of the static platform can be expressed as

$$\begin{aligned} R' &= R(\mathrm{x}, \alpha) * R(\mathrm{y}, \beta) * R(\mathrm{z}, \gamma) \\ &= \begin{bmatrix} 1 & 0 & 0 \\ 0 & \cos\alpha & -\sin\alpha \\ 0 & \sin\alpha & \cos\alpha \end{bmatrix} \begin{bmatrix} \cos\beta & 0 & \sin\beta \\ 0 & 1 & 0 \\ -\sin\beta & 0 & \cos\beta \end{bmatrix} \\ &\quad \times \begin{bmatrix} \cos\gamma & -\sin\gamma & 0 \\ \sin\gamma & \cos\gamma & 0 \\ 0 & 0 & 1 \end{bmatrix} \\ &= \begin{bmatrix} c\beta c\gamma & -s\gamma c\beta & s\beta \\ s\gamma c\alpha + s\alpha s\beta c\gamma & c\alpha c\gamma - s\alpha s\beta s\gamma & -s\alpha c\beta \\ s\alpha s\gamma - s\beta c\alpha c\gamma & s\beta s\gamma c\alpha + s\alpha c\gamma & c\alpha c\beta \end{bmatrix} \end{aligned} \tag{5}$$

In Equation (5), we use the letter s represents the function *sin*, and the letter c represents the function cos.

For Taylor's bone external fixator, the coordinates of the real-time pose of the dynamic platform coordinate system $Q{-}uvw$ in the static platform coordinate system $P{-}xyz$ can be expressed as (u_q, v_q, w_q), and its matrix form can be expressed as $q{=}\,[u_q, v_q, w_q]^T$. The rotation angle of the dynamic platform Q around the three-dimensional coordinate axis of the static platform is known as (α, β, γ). The six real-time pose parameters of the dynamic platform Q can be expressed as a set of 6-dimensional vectors $[u, v, w, \alpha, \beta, \gamma]$.

The optimal solution to the dynamic platform pose parameters in the two platform structures of the entire Taylor bone external fixator originates from the typical Stewart kinematics of the positive solution process [7]. By reading the specific scale values displayed in the six scale-marked retractable measuring rods and calculating the rotation matrix, the pose parameter of the dynamic platform Q corresponding to the known parameters can be found, and the pose parameter is unique. The rotation matrix of the dynamic platform coordinate system Q concerning the static platform coordinate

system P is set as $R^{'}$, and its rotated pose parameters are denoted by (α, β, γ).

After the displacement and angular offset happen between the two platforms, the origin of the coordinate system Q and the coordinate system P do not coincide in a geometric sense, and the direction of the positive axes of the two coordinate systems do not coincide. For each connection point N_i and M_i on the platform, the specific value of the telescopic rods can be calculated by the spatial geometric projection and the translation of the line segment.

Assuming that the cross-section of the fracture position is considered as the geometric center of the entire section, denoted as point A, the expression of point A in the static platform coordinate system $P - xyz$ is

$$^{P}A = R'^{Q}A + {}^{P}A_{Q} \tag{6}$$

Then the length of the extendable rod is represented by the vector

$$PA + AN_i = PM_i + M_iN_i, \quad i = 1, 2, \ldots, 6 \tag{7}$$

and

$$\overline{M_iN_i} = R'^{Q}n_i + a - {}^{P}m_i, \quad i = 1, 2, \ldots, 6 \tag{8}$$

Therefore, the rod length l_i of the retractable rod in the bone external fixator is equal to the norm of the vector $\overline{M_iN_i}$, which is the square root of the three-dimensional coordinates of the vector $\overline{M_iN_i}$, according to the definition of a norm in geometric mathematics, that is, $\left\|\overline{M_iN_i}\right\|$. In the dynamic platform Q, we can obtain the value of the rod length l_i,

$$l_i = \sqrt{(R'^{Q}n_i + a - {}^{P}m_i)^T(R'^{Q}n_i + a - {}^{P}m_i)} \quad \mathrm{i} = 1, 2, \ldots, 6 \tag{9}$$

In Equation (9), $^{Q}n_i$ is denoted as the parameter value at the hinges and dynamic ring connection point in the dynamic platform Q, and $^{P}m_i$ is denoted as the parameter value at the hinges and static ring connection point in the static platform P.

III. TSF KINEMATICS POSITIVE SOLUTION BASED ON MULTI-OBJECTIVE GENETIC ALGORITHM

A. ENCODING

Encoding is the primary problem to be solved when applying a genetic algorithm and is a key step when designing a genetic algorithm. The coding method affects the operation method of genetic operators such as crossover operator and variation operator, and it can be said that coding largely determines the efficiency of genetic evolution. There are two main types of coding for genetic algorithms, one is binary coding and the other is real coding. The study in this paper focuses on solving the optimal solution of a multidimensional system of primary equations, using a real number coding approach. In this paper, we try to align all the branches of the unknown Taylor skeleton and model them as a gene sequence.

B. GENERATE INITIAL POPULATIONS

In this paper, we assume that the size of the initial population is N. We can generate N individuals by random number as the initial gene sequence.

C. GENERATE THE FITNESS FUNCTION

In the kinematic positive solution problem of the Taylor bone external fixator, the core part of the multi-objective optimization problem is how to avoid excessive computation while ensuring the high efficiency of the algorithm calculation results, therefore it needs to calculate the fitness function value of each individual. By using the calculated fitness function values to stratify and filter all the population individuals N, and selecting individuals with better fitness for the next iterative solution work [12], among the set of all feasible solutions, the set of the fitness function values corresponding to the best fitness is called Pareto front [13]. The proposal of the Pareto front shows the adaptability of each n clear in the set in the current problem environment, and the workload of screening the optimal feasible solution is greatly reduced [14].

D. SELECTION OPERATION

After the range of the solution set of the optimal solution is further reduced, there are two solutions for how to choose among several feasible solutions without merit and comparison. The first one is to obtain the shared function habitat, calculating the Euclidean Distance between each individual in the Pareto front and the other individuals that need to be filtered, and sort each calculated Euclidean Distance value in descending order and use it as the progeny for the next iteration [15]. However, the parameters of the fitness function change in real-time according to the specific solution situation. For example, the fitness function obtained in the formula with different parameters is different, and the number of parameters of the function changes linearly with the dimension increase, which has extremely complex parameter requirements. It is obvious that this solution cannot be used in the kinematic positive solution problem of the Taylor bone external fixator. Therefore, in this paper, we choose the second solution by adding a scaled fitness selection probability to the multi-objective genetic algorithm to ensure the diversity of the feasible solution population, and the parameter values that are more consistent with Pareto's optimization theory are used as the parent population of the new generation of the genetic algorithm, whose selection probability is determined by the individual fitness function in the feasible solution set.

E. CROSSOVER OPERATION

Crossover is crucial in genetic algorithms, where a parent crossover can produce new offspring that inherit superior characteristics from the parent, essentially an exchange of information. The operation step is to randomly select two individuals in population N and combine the chromosomes of the two individuals to form a new offspring. In this paper,

we adopt the real number coding approach, and the specific steps are as follows:

a) We assume a crossover probability of pc and i iterations, with each iterative process first generating a random number rand;

b) If rand > pc, the crossover is abandoned, otherwise the crossover proceeds to the next step;

c) Randomly selecting two chromosomes, $c_i = (a_i)$, i = 1,2,…,6, $c_j = (a_j)$, j = 1,2,…,6, the real-time positional parameters of the dynamic platform Q can be expressed as a set of 6-dimensional vectors $[u, v, w, \alpha, \beta, \gamma]$, so the values here can be taken as 1,2,3…,6. A random number rand is generated by randomly selecting position k as the crossover position, and the swap operation for the two real numbers at position k is:

$$a_k = \text{rand} * b_k + (1 - \text{rand}) * a_k \tag{10}$$

$$b_k = \text{rand} * a_k + (1 - \text{rand}) * b_k \tag{11}$$

F. MUTATION OPERATION

We assume that the element X_i in the individual $X = (X_1, X_2, \ldots, X_N)$ mutates into a new element X_i' by the following equation:

$$X_i' = C_1 R_1 (X_i^b - x_i) + C_2 R_2 (X_i^b - x_i) \tag{12}$$

where: C_1, C_2 are both positive constants; R_1, R_2 are both random numbers on [0,1]; b is a parameter that controls the change in the size of element X_i.

The optimization of the optimal solution in this paper mainly relies on the selection and crossover operations, while the main role of the variational operation is to avoid the algorithm from falling into a local region of the search space, thus ensuring the global convergence of the algorithm. We assume that pm is the variation probability and a random number rand ∈ (0,1) is generated on each individual, and if rand < pm, then that individual needs to perform the above variation operation.

G. MULTI-OBJECTIVE GENETIC ALGORITHM EXECUTION STEPS

The multi-objective genetic algorithm can be described in pseudo-code, and the specific algorithm execution steps are shown in Figure 5 below:

Step 1: By measuring the initial pose parameters of the dynamic platform Q including the 3-D coordinates (u, v, w) of the geometric center point A and the rotation angle (α, β, γ) of the point A in the static platform coordinate system $P - xyz$, a set of vectors Si are noted, and $S_i = [u_i, v_i, w_i, \alpha_i, \beta_i, \gamma_i]$, $i = 1, 2, \ldots, n$;

Step 2: The least-squares theoretical calculation of the rod length scale value of the retractable rod obtained from the inverse solution and the known rod length scale value, when the residual of the two sets of data $\left|\sum_{i=1}^{6} V_i^2\right| < 2\sigma$, the program iteration ends and outputs the corresponding kinematics positive solution; The residual refers to the difference between the observed value and the theoretical value,

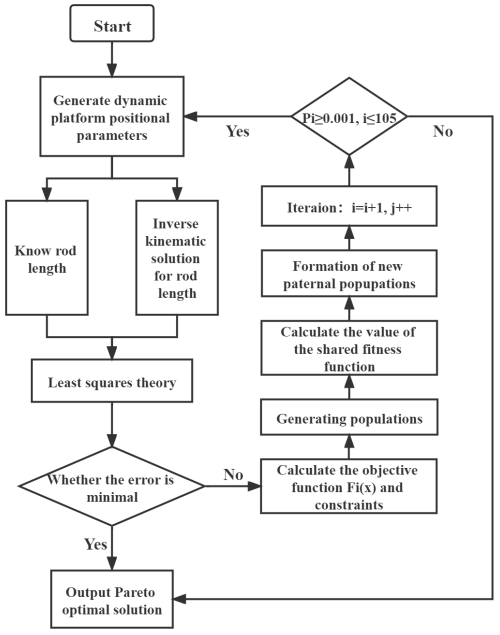

FIGURE 5. Flow chart of positive solution.

and the residual formula is a test criterion proposed by the theory of least squares. Otherwise, it is transferred to the multi-objective genetic algorithm for screening.

Step 3: Determine the objective function and constraints of the algorithm in the mathematical model, which can be written as

$$f_{\min} \quad (u, v, w, \alpha, \beta, \gamma)$$

$$s.t. \begin{cases} -97 < u < 97 \\ -97 < v < 97 \\ -158 < w < 158 \\ -90^\circ < \alpha < 90^\circ \\ -90^\circ < \beta < 90^\circ \\ -90^\circ < \gamma < 90^\circ \end{cases} \tag{13}$$

Step 4: According to the mathematical model of Taylor's bone external fixator platform structure in the objective function and constraints generated by all solutions of the system of Twelve 6-D primary nonlinear equations the initial population Si is noted in the multi-objective genetic algorithm, the composition of the dynamic platform Q will generate the possible initial pose parameters and S_i is a set of input 6-D vectors, $S_1 = [s_1\ s_2\ s_3\ s_4\ s_5\ s_6]^T$ and the first input pose parameter is S_2, and the next input pose parameters in order are $S_3, S_4, S_5, \ldots, S_i$, i = 2, i++;

Step 5: Calculate the functional fitness of the initial population S_i output from Step3; among the initial population S_i, compare the remaining population of individuals $S_2, S_3, \ldots, S_j$ with S_i in turn to obtain the dominant and non-dominant relationship between individuals, and i≠j, when the superiority of S_i is greater than S_j, S_i is the non-dominant individual

of the initial population; so let i = 1, j = 2, i = i + 1,j++; loop the algorithm in turn Step3, until all non-dominated individuals are found.

(a) Calculate the Euclidean distance between each individual x_i and the other remaining individuals x_j in the set of non-dominated individuals in the initial population obtained from Step 4.

$$\mathrm{d(i,j)} = \sqrt{\sum_{i=1}^{n} \left(\frac{x_i - x_j}{x_i^{\max} - x_i^{\min}}\right)^2} \tag{14}$$

x_i^{max} denotes the maximum value of the range of variation of individual x_i, x_i^{min} denotes the minimum value of individual x_i, final execution j = j + 1, i++;

(b) The shared function s representing the relationship between each individual x_i and the other remaining individuals x_j in the initial population is calculated, and its functional expression is

$$s(d(i,j)) = \begin{cases} 1 - \left(\frac{d(i,j)}{\sigma}\right)^{\alpha}, & \text{when } d(i,j) < \sigma \\ 0, & \text{others} \end{cases} \tag{15}$$

Among them

$$\sigma = \sqrt{\frac{\sum_{i=1}^{6} V_i^2}{n-t}} = \sqrt{\frac{\sum_{i=1}^{6} (S_i - S_i')^2}{n-t}} \tag{16}$$

t is the dimension of a set of vectors of the dynamic platform position parameters of the Taylor bone external fixator, here t = 6.

Then the functional fitness of each individual x_i in the nascent parent population is

$$P_i = \frac{f_i}{\sum_{i=1}^{n} f_i} = \frac{s\,(d\,(i,j))}{\sum_{i=1}^{n} s\,(d\,(i,j))} \tag{17}$$

And i = 1, j = 2; i = i + 1, j++, perform repeatedly until the fitness function value for each non-dominant individual in the population is obtained;

Step 6: Determine whether P_i is greater than 0.0001 and whether the number of iterations i is less than or equal to 105, if yes, go to Step2 and cycle in turn, otherwise, stop the cycle.

Step 7: At the end of the algorithm, output the Pareto optimal solution of the positive solution process for the dynamic platform Q of the Taylor bone external fixator corresponding to the pose parameters.

H. MULTI-OBJECTIVE GENETIC ALGORITHM FEASIBILITY VERIFICATION

Using the size of the Taylor Bone External Fixator component prepared in the laboratory and the maximum elongation scale values of the six retractable rod scales as reference bases, the circle radius of the dynamic platform is a_i= 97.0mm and the circle radius of the static platform is b_i= 97.0mm, select a vector set of initial attitude parameters of the dynamic platform Q, noted as S_1= [u_1, v_1, w_1, α_1, β_1, γ_1].

The maximum elongation value of the telescopic rod in the dynamic platform is 205mm, so the initial values of the rod lengths of the six telescopic rods are taken as l_1 = 183.92mm, l_2 = 185.22mm, l_3 = 182.89mm, l_4 = 156.62mm, l_5 = 157.16mm, l_6 = 180.37mm.

The calculation is performed using the multi-objective genetic algorithm proposed above, the value of the pose parameter S_1 = [u_1, v_1, w_1, α_1, β_1, γ_1] of the dynamic platform Q corresponds to the initial rod length vector set L_1 = [183.92, 185.22, 182.89, 156.62, 157.16, 180.37].

For the method of estimating the accuracy of the algorithm fit between the values obtained by the multi-objective genetic algorithm, this test takes the Root Mean Squared Error (RMSE) as judging the reasonableness of the two sets of data. The numerical analysis module of standard error in statistical theory is extremely important, which can screen out a set of abnormal data in the comparative data, and can filter out the unsatisfactory pose parameters of the dynamic platform kinematics positive solution, the specific calculation formula is

$$RMSE = \sqrt{\frac{\sum_{i=1}^{n} \left(X_{obs,i} - X_{\mathrm{mod}\,el,i}\right)^2}{n}} = \sqrt{\frac{P_i}{n}} \tag{18}$$

where the algebraic expression for P_i is given in Equation (17). For the initial rod length array L_1 of the dynamic platform Q in this test, the data are calculated for 10 repetitions. Each group of pose parameters, the function fitness value P_i and Root Mean Squared Error (RMSE) is calculated by the positive solution of the multi-objective genetic algorithm, as shown in Table 1.

For the pose parameters of the 10 sets of dynamic platform Q corresponding to the vector group L_1 of the telescoprod length, the errors between the values of angular offset α_i, β_i, and γ_i of each group basically remain within ± 0.1, and the errors between the Cartesian coordinate system (u_i, v_i, w_i) of each group basically have stable performance fluctuating between ± 1, except for the 9th group that has a small deviation from the other groups. All the other groups are available and the accuracies are less than 0.01, and the standard error values of each group are stable basically remaining within $2.5 \times 10^{-2} \pm 4 \times 10^{-3}$.

As for the feasibility of the algorithm, it is verified by setting up experimental cases that the optimal solution of the pose parameters is selected by multiple positive solutions without abnormal data, and the multi-objective genetic algorithm with the introduction of adaptation selection probability P_i and standard error calculation $RMSE_i$ performs well in the mathematical model of the Taylor bone external fixation machine platform mechanism, and the whole algorithm process is solved with high efficiency, high accuracy, and stable performance of the pose parameters. It well avoids the hot machine learning and deep learning in the processing of big data models. For the surgical operation of fracture correction using Taylor bone external fixation, its multi-objective genetic algorithm is enough to meet the requirements of data

TABLE 1. Data of related parameters in 10 groups of tests in positive solution process.

u_i/mm	v_i/mm	w_i/mm	α_i (°)	β_i (°)	γ_i (°)	P_i	$RMSE_i$
20.128	-50.792	90.724	30.5	-24.5	36.5	7.13x10^{-3}	2.67x10^{-2}
20.595	-49.819	91.087	30.4	-24.5	35.7	6.48 x10^{-3}	2.54 x10^{-2}
19.524	-50.398	90.195	30.5	-24.4	36.5	7.08 x10^{-3}	2.66 x10^{-2}
19.896	-50.407	89.726	30.5	-24.3	36.3	5.72 x10^{-3}	2.39 x10^{-2}
20.821	-51.201	91.011	29.9	24.4	36.5	7.39 x10^{-3}	2.71 x10^{-2}
20.706	-49.791	90.452	31.1	24.4	35.6	6.41 x10^{-3}	2.53 x10^{-2}
20.551	-51.004	89.709	30.5	23.8	36.4	6.81 x10^{-3}	2.61 x10^{-2}
20.516	-50.176	90.179	29.8	24.3	36.3	7.59 x10^{-3}	2.75 x10^{-2}
21.283	-49.807	91.167	30.6	23.5	36.4	4.82 x10^{-3}	2.20 x10^{-2}
20.610	-50.026	90.031	30.4	24.3	36.6	6.93 x10^{-3}	2.63 x10^{-2}

accuracy, which can be solved by the positive solution process in the dynamic platform in the mathematical model.

Among the 10 sets of pose parameter data obtained from the positive solution of the mathematical model, any one set of data is selected for the inverse solution of the model, and the inverse solution formula is

$$l_i = \sqrt{l_{xi}^2 + l_{yi}^2 + l_{zi}^2} \tag{19}$$

The first set of parameters S1 = [20.128 −50.792 90.724 30.5 − 24.536.5] is chosen as the substitution value for the inverse solution of the model, and the rod length of the extendable rod $L_1^{'}$ is obtained by the inverse solution modeling process, that is

$$L_1^{'} = [182.73,\ 184.53,\ 179.85,\ 156.67,\ 156.14,\ 178.81].$$

The correlation test between the data is performed using the Pearson correlation coefficient for the two sets of data L_1 and $L_1^{'}$ that are obtained. It can reflect the closeness of the correlation between two sets of data L_1 and $L_1^{'}$. Its Pearson correlation coefficient is calculated by the formula

$$r\left(L_1, L_1'\right) = \frac{Cov(L_1, L_1')}{\sqrt{Var\left[L_1\right] Var\left[L_1'\right]}} \tag{20}$$

where $Cov(L_1, L_1^{'})$ denotes the covariance between the variables L_1 and $L_1^{'}$, $Var[L_1]$ and $Var[L_1^{'}]$ denote the variance of L_1 and $L_1^{'}$ respectively. The specific values of each component are calculated algebraically as shown in Table 2 below:

After reviewing the information, the strength levels of Pearson's correlation coefficient are shown in Table 3:

Combining Table 3 with Table 2, the initial rod length value of the Taylor Bone External Fixator telescopic rod and the rod length value obtained from the inverse solution are tested by Pearson's correlation coefficient $r(L_1, L_1^{'})$, and the result is 0.955, which is within the range of 0.8-1.0 confirming a strong correlation between the data, therefore, both sets of data are normal and no abnormal data are generated. For bone surgery, the precision of the instruments is not particularly high and the error is within the acceptable range, so using the multi-objective genetic algorithm as a method to solve the mathematical model of Taylor's bone external fixation retainer platform is feasible and efficient.

To verify the superiority of the proposed multi-objective genetic algorithm compared with other methods, we compare the proposed multi-objective genetic algorithm with the traditional numerical method, and here we take the Newton-Raphson method as an example to consider the superiority of the algorithm in a more intuitive way from the dimension of the accuracy of parameter solution.

The Newton-Raphson method is an extremely basic algorithm for solving nonlinear problems, and its basic idea is to linearize the nonlinear problem one at a time to form an iterative procedure. Like the multi-objective genetic algorithm

TABLE 2. Partial substitution of pearson correlation coefficient (Unit: mm).

$E(L_1)$	$E(L_1')$	$E(L_1, L_1')$	$Cov(L_1, L_1')$	$Var[L_1]$	$Var[L_1']$	r(%)
174.363	173.205	30334.615	134.072	154.91	127.34	0.955

TABLE 3. Pearson correlation coefficient grade comparison table.

Correlation level	Extremely strong correlation	Strong correlation	Moderate correlation	Weak correlation	No correlation
Range of values	0.8-1.0	0.6-0.8	0.4-0.6	0.2-0.4	0.0-0.2

TABLE 4. Positive solution results with RMSE accuracy.

Algorithm	u_i/mm	v_i/mm	w_i/mm	α_i (°)	β_i (°)	γ_i (°)	$RMSE_i$
Algorithm of this paper	26.512	30.223	74.589	15.5	10.4	15.2	$2.67\text{x}10^{-2}$
Newton-Raphson	16.546	34.981	66.854	14.3	9.6	15.0	$2.67\ \text{x}10^{-2}$

TABLE 5. Telescopic rod length for different algorithms.

Algorithm	Rod 1	Rod 2	Rod 3	Rod 4	Rod 5	Rod 6
Algorithm of this paper	132.1426	143.8992	113.6485	162.8639	171.6783	151.8687
Newton-Raphson	126.2218	137.8784	106.8205	158.3266	161.1311	140.4377
Benchmark data	130	143	112	161	169	152
Absolute value of error	2.1426/ 3.7782	0.8992/ 5.1216	1.6485/ 5.1795	1.8639/ 2.6734	2.6783/ 7.8689	0.1313/ 11.5623

solution process, we need to solve the positional values (u, v, w, α, β, γ) of the dynamic platform under the precondition that the lengths of the six stubs of the Taylor frame are known. We randomly use the same set of strut lengths [130, 143, 112, 161, 169, 152] of the Taylor frame as the initial data source, which we refer to as the baseline data. We use the positive solution procedure of this scheme to compare with the Newton-Raphson method and limit the RMSE to 2.67×10^{-2}, and the comparison data are shown in Table 4 below:

We obtained the telescopic rod lengths of the six Taylor frames corresponding to the two sets of solutions based on the positive solution results in Table 4 and using the inverse solution Equation (9), as shown in Table 5 below.

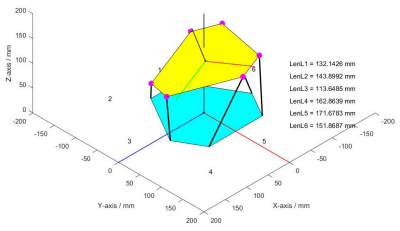

FIGURE 6. The algorithm in this paper simulates the correction chart.

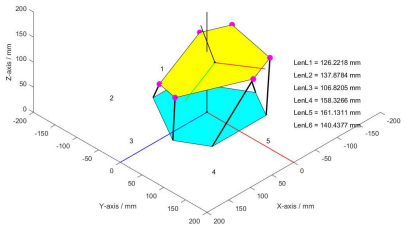

FIGURE 7. Newton-Raphson simulation correction chart.

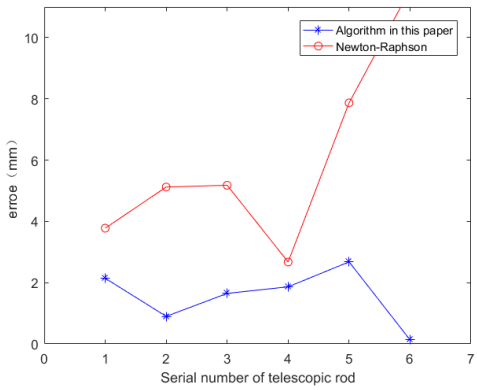

FIGURE 8. Error comparison chart.

The lengths of the telescoping rods solved from the same set of benchmark data are worth the variability is relatively large, and the corrected graphs of the experimental simulation are shown in Figure 6, Figure 7. As shown in Figure 6 and Figure 7, we can visually see that although the difference between the two algorithms is only on the order of millimeters in the installation parameters of the struts, we can see the difference in attitude between the two correction charts of the experimental simulation with the naked eye. Due to the high requirements of the Taylor frame in clinical orthopedic applications for the installation parameters of the struts, and the long orthopedic cycle, once the pre-installation parameters are inaccurate, it will have an increasing impact on the later treatment of skeletal patients. From this perspective, we aim to improve the accuracy of the parameters required for the installation of the Taylor frame as much as possible, and to promote the application of the Taylor frame in actual clinical treatment.

In the simulation correction process, we draw the error comparison graph shown in Figure 8 below according to

the error values in Table 5, from which it can be seen that the accuracy of the calculation of the required parameters for TSF proposed in this paper is much higher than that of the traditional numerical method. Among them, although the installation accuracy of Rod 4 rod has a smaller improvement compared with the accuracy of other struts, it also has about 0.8 mm accuracy improvement.

IV. SIMULATION TEST OF TIBIAL FRACTURE WITH ORTHOPEDIC SYSTEM

The orthopedic system is designed based on the multi-objective genetic algorithm combined with the kinematic model of the Taylor bone external fixator, which provides the algorithm and technical environment to support the fracture correction simulation test. In this paper, we use the orthopedic prescription data generated by the system to simulate the orthopedic test on the fracture end of the human tibia, to understand the orthopedic method and steps by simulating the whole process of orthopedic correction on the fracture segment of the tibia, and to verify the accuracy and clinical feasibility of the prescription data generated by the orthopedic system in the test.

A. DEVELOP THE TEST ENVIRONMENT AND THE STEPS

The tools used in the testing hardware environment are the six degrees of freedom type Taylor Bone external fixation kit produced by Beijing Ruilong Medical Device Co, in which the dynamic platform and static platform both adopted the rigid structure platform with an internal diameter of 194mm, the range of the retractable rod is 50mm-300mm, the type of tibial segment fixation pin is selected as the Kirsch pin, and the length of the tibia is 40cm and the circumference is 11cm, which meets the requirements of the external fixator for the tibia. The tools of the software environment include OriginPro and the orthotic system platform. The whole experimental process includes five parts: setting up the experimental environment, solving the pose parameters, generating the correction prescription data, manually simulating the correction and verifying the experimental effect. The specific test process is shown in Figure 9 of the following structure.

B. SOLVING FOR DISTORTIONAL POSE PARAMETERS

1) MARKING OUT IMAGE FIXATION POINTS

Before marking the fixed point, the deformity shape of the tibial fracture segment suitable for the test equipment should be selected. Since the inner diameter of the test equipment has been fixed, the shape of the fracture segment with more severe deformity should not be selected. In this study, clinical data of 2 cases with different degrees of tibial fracture deformity positions are selected as the test sample data, which are recorded as the test sample data of group i, i = 1,2, respectively. After the tibial segment deformity shape is determined, the truncated tibia should be passed through the hole of the bone model with Kirschner wire according to the pre-selected deformity shape and fixed on the fixator of the platform. Digital images are taken on the tibia of the patient, in which the angle of the telescopic rod numbered 1 and 6 is selected to shoot the anteroposterior digital images of the tibia, and then the patient is rotated counterclockwise by 90° to shoot the lateral digital images. The anteroposterior and lateral digital images of the patients are imported into the visualization window of Digitizer function in OriginPro software, and a reasonable two-dimensional coordinate system is developed according to the specific positions of the fixator and tibial segment in the digital images, and a fixed-point coordinate model based on Digitizer function is established.

2) SOLVING FOR DISTORTIONAL POSE PARAMETERS

Choose the geometric center of tibial fracture end on the cross-section as point A, circle a point B, the geometric center dynamic platform on the surface of the tibia bone fracture end designates point C, the geometric center of the end of the tibia in cross-section designates point D, ∠ABC for the tibia and the deformation of the z-axis offset Angle $\angle\Upsilon$, because of the tibia and the Angle between the axis u dynamic platform and tibia and the Angle between the axes x are similar, so it is $\angle\beta$. The four selected fixed points A, B, C and D are calculated in the model, and the coordinate values of each fixed point in the Digitizer function model are counted. The morphology diagram of the tibial fracture and the corresponding fixed points in the digital image in the coordinate mode1 are shown in Figure 10.

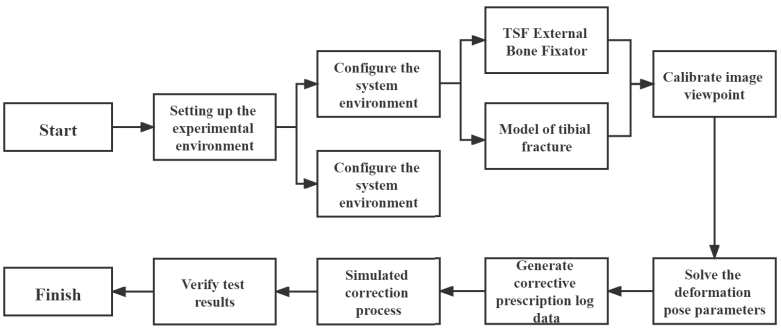

FIGURE 9. Test flow chart.

TABLE 6. Coordinate of digital image fixed point in model.

point	A	B	C	D
Group 1 fixed point coordinates (mm)	(-7.826,109.982)	(10.45,145.599)	(5.85,107.152)	(23.663,178.564)
	A'	B'	C'	D'
	(-31.62,121.932)	(-0.191,178.784)	(-0.191,119.102)	(31.775,205.589)
Group 2 fixed point coordinates (mm)	A	B	C	D
	(-24.512,134.292)	(5.550,199.928)	(-0.577,133.710)	(12.252,204.372)
	A'	B'	C'	D'
	(-23.652,135.513)	(-3.868,186.940)	(-0.046,134.447)	(4.010,200.486)

TABLE 7. The solution results of relative pose parameters in each group of sample data.

	u (mm)	v (mm)	w' (mm)	w'' (mm)	α (◦)	β (◦)	γ (◦)
S_1	-31.625	-7.826	2.830	2.830	39.706	54.326	-12.391
S_2	-23.652	-24.512	1.066	1.066	70.510	19.951	-55.810

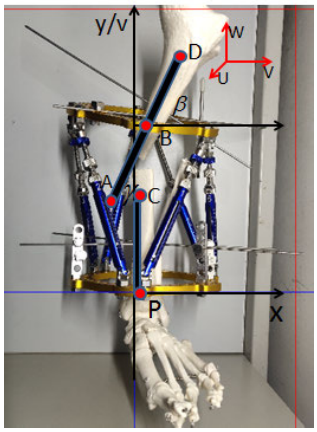

FIGURE 10. Fixed point coordinate model of positive image.

According to the fixed point coordinates and pose parameters of Experiment 1 and Experiment 2 in the model shown in Table 6 and Table 7 below, the position and pose parameters S_i, i = 1,2, and $S_i = [u\ v\ w\ \alpha\ \beta\ \Upsilon]$ of the upper tibia fracture end in the dynamic platform coordinate system Q_{-uvw} are obtained by using the above formula.

The values in the test sample data of w of two groups can be known from Table 7 that each group of $w' = w''$, so according to the parameter determination conditions of fixed coordinate model validation, sample test data of each deformity pose parameters of the solving result is correct and effective, parameter values can be input to Taylor bone external fixator orthopedic system and participate in the process of TSF action platform kinematics solution.

C. DEVELOPING A PRESCRIPTION FOR CORRECTION

The six deformity pose parameters are obtained by the fixed-point coordinate model, and the scale value of each retractable rod l_i is adjusted according to the corresponding parameter values during the test, and the pose and shape of the tibial segment on the external fixation platform is obtained. Before making the correction prescription in the system, the installation parameters of the 194mm internal diameter Taylor bone external fixator kit, including the median height of the rigid body ring structure and hinge ball distance, need to be calculated.

The straight-line distance between the hinge ball and the center of any two holes used to fix the hinge in the outermost part of the rigid body structure ring of the movable platform of the external phalangeal fixator is denoted as $L_{distance}$, and the unit is millimeter. The structural diagram of the hinge ball is shown in Figure 11. According to the vernier caliper measurement, the movable platform hinge ball distance of 194mm TSF external bone fixator is selected as 25mm in this experiment.

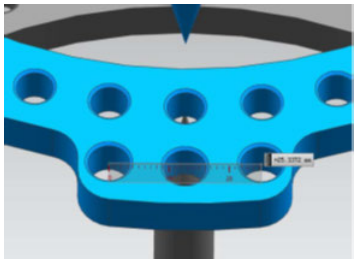

FIGURE 11. Schematic diagram of hinge ball distance of the dynamic platform.

Median height refers to the geometric distance between the center of the fixed hinge between the dynamic ring and the static ring after the bone segment is adjusted in place in the fixator platform, we use h_{mid} to denote the median height, and the formula is expressed as

$$h_{mid} = h = a + b - 2c \tag{21}$$

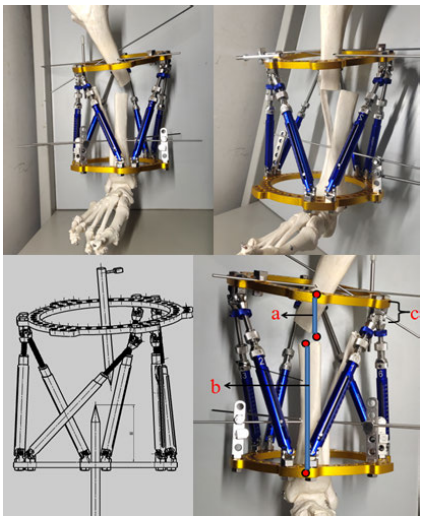

FIGURE 12. The schematic diagram of 2 cases of abnormal position and some parameters in the fixator structure.

Since the median height is defined as the height of the bone segment after it is adjusted in place in the platform, the distance of the upper tibia segment A is measured at the initial state of the platform, where A represents the geometric distance between the section of the upper tibia and the center of the circle on the lower surface of the dynamic ring. When the tibia segment is in the adjusted state, the mounting parameter b is measured, where b represents the geometric distance from the section of the lower tibia to the center of the circle on the upper surface of the static ring. The measurement results of distance A and distance B are different in different deformity poses. C is the hinge fit height, specifically referring to the vertical distance between the center of the Hook hinge axis and the surface of the dynamic platform. According to the actual measurement, the installation parameters of the TSF retainer in the first test are a = 51mm, b = 116mm, and the hinge fit height c = 24.2mm, so the calculated value of h_{mid} is 118.6mm. The installation parameters of the TSF retainer in the second test a = 43mm, b = 116mm, and the hinge fit height c = 24. 2mm, so the calculated value of h_{mid} is 110.6mm.

The correction period T represents the number of days to be adjusted, and the longer the correction period is, the higher the accuracy of correction prescription data value calculated by the orthopedic system is. In this test, T = 100. Corrective interval t means the length value of the retractable rod, which is adjusted once every few days. The specific value is calculated by the degree of injury at the fracture site of the patient. The greater the degree of fracture, the greater the value t of the selected interval is; in this experiment, t = 1.

After all the installation parameters in the system are calculated and confirmed to be correct, the user logs into the orthopedic system platform according to the account and password assigned by the super administrator and fills in the patient history information, each installation parameter of the device

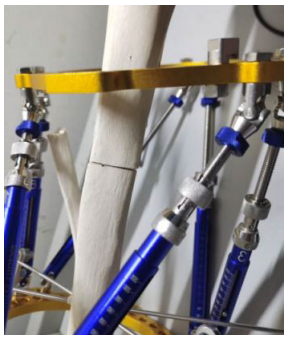

FIGURE 13. Cross-section of tibial posterior fracture correction.

and the postural deformity parameters in Table 7 following the instructions and precautions for the use of each functional module of the orthopedic system, and the specific values of each variable and deformity parameter are compared as shown in (a) and (b) in Table 8 below, respectively. After checking the input data and confirming it is correct, click ''Add'' and ''Prescription'' buttons to generate prescription data corresponding to the morphology of the tibial fracture segment of the two groups in the orthopedic system.

D. ANALYSIS OF TEST RESULTS

Taylor bone external fixator adjusting system based on the input segment tibia abnormalities in patients with pose parameters are calculated to generate correct prescription data in predistortion cycle log report. This part of the log data generated test orthopedic system of the display is shown in Figure 14, the data displayed in green indicates that the correction data is out of the range of the current retractable rod and needs to be replaced with another size of the retractable rod to match the current prescription data.

Calculate according to the system to generate the correct prescription of log data, click the correct parameter management interface to view the correct details every day, to adjust the predistortion cycle in each experiment group 6 telescopic rod length value and be able to response to the sudden situation in the later in the process of clinical orthopedic, need to purpose the edit log and add notes, until the end of 2 groups of the simulated correction process. Part of the experimental group after the correction of the tibia in the position of TSF holder form is shown in Figure 13, tibial fractures can strictly coincidence, the section will correct after tibial form into a digital image according to the measured analog correct experiment 1 and 2 on the tibia bone, and the bone at the center of the cross-section of the axis offset angle is 0.9° and 0.7°, fracture end section overlap, corrective effect is good.

Since the median height h_{mid} of the tibial segment without fracture is fixed in the dynamic platform of the Taylor external bone fixator, the median height h_{mid} can be used as a standard condition to judge whether the results of the simulated correction test for tibial fracture are valid. During the simulation test, the median height h_{mid} of each group of

TABLE 8. Comparison of parameters in the test.

Variables	Mounting position	Hinge ball distance	Cycle T	interval t	a_i	b_i	$l_{i\max}$	$l_{i\min}$
Numerical values	Tibia	25mm	100 days	1/day	97mm	97mm	205mm	145mm
Variables	l_1	l_2	l_3	l_4	l_5	l_6	h_{mid}	Remarks
Group 1	146.55	157.89	174.56	201.05	204.50	149.70	118.60	None
Group 2	145.00	179.10	173.85	203.10	181.50	162.50	104.80	None

(a)

Deformation parameters	X-axis displacement Error u	Y-axis displacement Error v	Z-axis displacement Error w	X-axis offset Corner α	Y-axis offset Corner β	Z-axis offset Corner γ
Group 1	-31.625	-7.826	2.83	39.706	54.326	-12.391
Group 2	-23.652	-24.512	1.066	70.510	19.951	-55.810

(b)

id	Patitent Name	Fix Position	Adjust date	Pole 1	Pole 2	Pole 3	Pole 4	Pole 5	Pole 6
9564	Mr. Wang	Tibia	2020-10-25	146.55	157.89	174.56	201.05	204.5	149.7
9618	Mr. Wang	Tibia	2020-10-26	147.43313702	158.39360350	174.42121757	202.02957267	205.20922254	151.51510406
9550	Mr. Wang	Tibia	2020-10-27	148.32784924	158.89383201	174.28396547	203.00834638	205.92457696	153.33098368
9573	Mr. Wang	Tibia	2020-10-28	149.23383529	159.39065534	174.14835162	203.98623607	206.64593980	155.14752360
9590	Mr. Wang	Tibia	2020-10-29	150.15099351	159.38404788	174.01448449	204.96335717	207.37318702	156.96461106
9571	Mr. Wang	Tibia	2020-10-30	151.07917208	160.37398356	173.33247297	205.93952551	203.10619401	158.78213564
9543	Mr. Wang	Tibia	2020-10-31	152.01821911	160.86044034	173.75242640	206.91475737	208.84483566	160.59998914
9574	Mr. Wang	Tibia	2020-11-01	152.96798276	161.34340019	173.62445457	207.88901943	209.58898646	162.41806555

FIGURE 14. Partial correction prescription data.

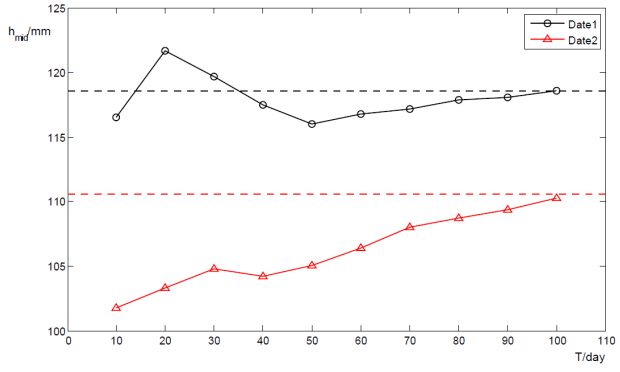

FIGURE 15. The change trend of h_{mid} in each experimental group.

simulated correction tests is recorded every 10 days, and the median height value of each group of data is compared with the median height value under the condition of no fracture, and the curve diagram of the change trend of the median height h_{mid} of the two groups of test data with time T is drawn, as shown in Figure 15.

By analyzing the h_{mid} curves of the median height of the tibia in each experimental group, it can be seen that the h_{mid} changes of the two experimental samples are infinitely close to the h_{mid} value of the tibia without fracture, which indicates that the correction data generated by the system is accurate and effective, and the healing state and correction effect of the bone section is good, reaching the expected effect of the experiment.

V. CONCLUSION

In this paper, we analyze the hardware structure of TSF, establish a reasonable platform structure model and analyze the positive and negative solution process of TSF dynamic and static platform. We perform the kinematic solution to the kinematic inverse solution process by the vector solution method, and obtain the formula for the kinematic inverse solution problem by projecting the geometry of the dynamic platform and selecting the appropriate line segments for vector derivation, and use this formula to verify the feasibility of the experimental later scheme in this paper.

By studying and analyzing the positive solution process of the TSF kinematic platform, the multi-objective optimization problem with 12 6-dimensional constraints is solved by drawing on the multi-objective genetic algorithm, and the results show that the optimal solutions of the initial positional parameters obtained multiple times are extremely correlated. In this paper, a genetic algorithm is creatively introduced into

the parameter solving process of TSF for the first time, and the superiority of this scheme is analyzed by experimental comparison. The solution of this paper has better accuracy than the Newton-Raphson method, which is a traditional numerical method, and can better promote the application of TSF in the field of orthopedic surgery.

Simulation tests on tibial fractures show that the results of solving the posture angle information are stable, although there is some error in the coordinate position information, the error of each calculation is stable within a certain range and the difference is small. It is acceptable for the kinematic positive solution of the platform, indicating that the method can be used for the solution of the platform poses.

In this paper, the Taylor Bone External Fixator Orthopedic system was designed based on multi-objective genetic algorithm in the later stage of the experiment, and the experimental case of human tibial fracture was used to simulate the fracture correction process by using the orthopedic system platform to generate the correction prescription data within the predetermined correction cycle, and the experimental results showed that the reunion status of the tibial fracture end section was well performed. This paper provides a solution for the development of a precision treatment platform for orthopedic medicine while validating the constructability of the correction prescription data generated by the orthopedic system for the treatment of tibial fractures in the trial.

The genetic algorithm can well solve the effect of errors brought by TSF in the actual sampling, and the genetic algorithm has high global and excellent adaptability. Accordingly, the disadvantage is the slow convergence rate. And, the genetic algorithm generates N individuals at random to form an initial solution during initialization, which may bring bad random effects. In this paper, a set of solutions is derived by least-squares theory and added to this initial population as an initial qualification of the initial population. Of course, we can also try to combine the simulated annealing algorithm to improve the finding speed and accuracy of the parameter solution of this scheme.

REFERENCES

[1] K. Panagiotopoulos, P. N. Soucacos, D. S. Korres, G. Petrocheilou, A. Kalogeropoulos, E. Panagiotopoulos, and A. B. Zoubos, "Anatomical study and colour Doppler assessment of the skin perforators of the anterior tibial artery and possible clinical applications," *J. Plastic, Reconstructive Aesthetic Surg.*, vol. 62, no. 11, pp. 1524–1529, Nov. 2009.

[2] R. Rambani, R. Raman, J. Singh, Z. Hashim, and H. K. Sharma, "The relationship between time to surgical debridement and incidence of infection in grade III open fractures," *Strategies Trauma Limb Reconstruction*, vol. 7, no. 1, pp. 33–37, Apr. 2012.

[3] D. J. Henderson, J. L. Rushbrook, P. J. Harwood, and T. D. Stewart, "What are the biomechanical properties of the Taylor spatial frame?" *Clin. Orthopaedics Rel. Res.*, vol. 475, no. 5, pp. 1472–1482, 2017.

[4] D. Dammerer, K. Kirschbichler, L. Donnan, G. Kaufmann, M. Krismer, and R. Biedermann, "Clinical value of the Taylor spatial frame: A comparison with the Ilizarov and orthofix fixators," *J. Children's Orthopaedics*, vol. 5, no. 5, pp. 343–349, Oct. 2011.

[5] L. Rolland and R. Chandra, "The forward kinematics of the 6–6 parallel manipulator using an evolutionary algorithm based on generalized generation gap with parent-centric crossover," *Robotica*, vol. 34, no. 1, pp. 1–22, Jan. 2016.

[6] S. Cheng, Y. Liu, and H. Wu, "A new approach for the forward kinematics of nearly general Stewart platform with an extra sensor," *J. Adv. Mech. Des., Syst., Manuf.*, vol. 11, no. 2, pp. 32–34,2017.

[7] Z. Xie, C. Feng, and C. Wang, "Kinematics positive solution of 6-PSS parallel robot based on BP neural network," *J. Mach. Des.*, no. 10, pp. 36–39, 2014.

[8] C. J. Jordan, R. Y. Goldstein, T. M. McLaurin, and A. Grant, "The evolution of the Ilizarov technique: Part 1: The history of limb lengthening," *Bull. Hospital Joint Diseases*, vol. 71, no. 1, pp. 89–95, 2013.

[9] T. Bb, R. Shanmugam, R. Gunalan, Y. P. Chua, G. Hossain, and A. Saw, "A biomechanical comparison between Taylor's spatial frame and Ilizarov external fixator," *Malaysian Orthopaedic J.*, vol. 8, no. 2, pp. 35–39, 2014.

[10] A. Khunda, M. Al-Maiyah, W. G. P. Eardley, and R. Montgomery, "The management of tibial fracture non-union using the Taylor spatial frame," *J. Orthopaedics*, vol. 13, no. 4, pp. 360–363, Dec. 2016.

[11] H. Ren and P. Ben-Tzvi, "Learning inverse kinematics and dynamics of a robotic manipulator using generative adversarial networks," *Robot. Auton. Syst.*, vol. 124, pp. 387–389, Feb. 2020.

[12] Y. Elbatrawy, I. E. A. Abuomira, F. Sala, G. Lovisetti, S. Alati, and D. Capitani, "Distraction osteogenesis for tibial nonunion with bone loss using combined Ilizarov and Taylor spatial frames versus a conventional circular frame," *Strategies Trauma Limb Reconstruction*, vol. 11, no. 3, pp. 153–159, Nov. 2016.

[13] S. Sokucu, "Perioperative versus postoperative measurement of Taylor spatial frame mounting parameters," *Acta Orthopaedica et Traumatologica Turcica*, vol. 48, no. 5, pp. 491–494, 2014.

[14] H. S. An, J. H. Lee, C. Lee, T. Seo, and J. W. Lee, "Geometrical kinematic solution of serial spatial manipulators using screw theory," *Mechanism Mach. Theory*, vol. 116, pp. 404–418, Oct. 2017.

[15] A. El-Sherbiny, A. Mostafa Elhosseini, and Y. Amira Haikal, "A comparative study of soft computing methods to solve inverse kinematics problem," *Ain Shams Eng. J.*, vol. 8, pp. 12–15, Jan. 2017.

JIANMIN GUO was born in 1978. He received the bachelor's degree in nonwovens science and engineering, the M.S. degree in computer science and technology, and the Ph.D. degree in computer nondestructive testing from Tiangong University, Tianjin, China, in 2001, 2006, and 2014, respectively. In 2006, he joined the Information Center, Tiangong University. In 2018, he was an Associate Professor with Tiangong University. He has been the Vice Dean of Office of network security and information technology, since 2020. He has authored or coauthored more than ten technical articles and edited the book *Practical Application Course of Artificial Intelligence Development*. He received more than eight software copyrights. His research interests include computer application and artificial intelligence.

JIALONG SU was born in 1993. He is currently pursuing the M.S. degree. His research interests include computer application and the Internet of Things.